Cell Transplantation
2019, Vol. 28(7) 907–923

DOI: 10.1177/0963689719844260
journals.sagepub.com/home/cll
SAGE

Quantitative Analysis of SSEA3+ Cells from Human Umbilical Cord after Magnetic Sorting

Zikuan Leng[1,2], Dongming Sun[2], Zihao Huang[3], Iman Tadmori[2], Ning Chiang[2], Nikhit Kethidi[2], Ahmed Sabra[2], Yoshihiro Kushida[4], Yu-Show Fu[3], Mari Dezawa[4], Xijing He[1], and Wise Young[2]

Abstract

Multilineage-differentiating stress-enduring (Muse) cells are a population of pluripotent stage-specific embryonic antigen 3 (SSEA3)+ mesenchymal stem cells first described by Mari Dezawa in 2010. Although some investigators have reported SSEA3+ mesenchymal cells in umbilical cord tissues, none have quantitatively compared SSEA3+ cells isolated from Wharton's jelly (WJ) and the cord lining (CL) of human umbilical cords (HUCs). We separated WJ and the CL from HUCs, cultured mesenchymal stromal cells (MSCs) isolated from these two tissues with collagenase, and quantified the percentage of SSEA3+ cells over three passages. The first passage had 5.0% $\pm$ 4.3% and 5.3% $\pm$ 5.1% SSEA3+ cells from WJ and the CL, respectively, but the percentage of SSEA3+ cells decreased significantly ($P < 0.05$) between P0 and P2 in the CL group and between P0 and P1 in the WJ group. Magnetic-activated cell sorting (MACS) markedly enriched SSEA3+ cells to 91.4% $\pm$ 3.2%. Upon culture of the sorted population, we found that the SSEA3+ percentage ranged from 62.5% to 76.0% in P2–P5 and then declined to 42.0%–54.7% between P6 and P9. At P10, the cultures contained 37.4% SSEA3+ cells. After P10, we resorted the cells and achieved 89.4% SSEA3+ cells in culture. The procedure for MACS-based enrichment of SSEA3+ cells, followed by expansion in culture and a re-enrichment step, allows the isolation of many millions of SSEA3+ cells in relatively pure culture. When cultured, the sorted SSEA3+ cells differentiated into embryoid spheres and survived 4 weeks after transplant into a contused Sprague-Dawley rat spinal cord. The transplanted SSEA3+ cells migrated into the injury area from four injection points around the contusion site and did not produce any tumors. The umbilical cord is an excellent source of fetal Muse cells, and our method allows the practical and efficient isolation and expansion of relatively pure populations of SSEA3+ Muse cells that can be matched by human leukocyte antigen for transplantation in human trials.

Keywords

spinal cord injury, cell transplantation, immune-tolerant, SSEA3+, mesenchymal stromal cells, magnetic-activated cell sorting

[1] Department of Orthopedics, Second Affiliated Hospital of Xi'an Jiaotong University, Xi'an, China
[2] W.M. Keck Center for Collaborative Neuroscience, Rutgers, the State University of New Jersey, Piscataway, New Jersey, USA
[3] Department of Anatomy and Cell Biology, School of Medicine, National Yang-Ming University, Taipei
[4] Department of Stem Cell Biology and Histology, Tohoku University Graduate School of Medicine, Sendai, Japan

Submitted: February 6, 2019. Revised: February 28, 2019. Accepted: March 12, 2019.

Corresponding Authors:
Xijing He, Department of Orthopedics, Second Affiliated Hospital of Xi'an Jiaotong University, No. 157, West Fifth Road, Xi'an 710004, China.
Email: xijing_h@vip.tom.com

Wise Young, W.M. Keck Center for Collaborative Neuroscience, Rutgers, The State University of New Jersey, 604 Allison Road, D-251, Piscataway, NJ 08854, USA.
Email: wisey@mac.com

Table 1. Antibodies Used in This Study.

Antibody	Host and Reaction	Dilution	Manufacture	Catalog #	Usage
SSEA3	Rat anti-human	1:20	Thermo Fisher Scientific	MA1-020	Immunocytochemistry, Flow cytometry, MACS
IgMκ	Rat, isotype	1:5	BD Pharmingen	550342	Immunocytochemistry, Flow cytometry
CD105	Rabbit anti-human	1:500	Thermo Fisher Scientific	PA5-12511	Immunocytochemistry
Ki-67	Rabbit anti-human	1:500	Abcam	ab16667	Immunocytochemistry
STEM 101	Mouse anti-human	1:500	Takara Bio, Inc.	Y40400	Immunocytochemistry
Hoechst 33342	Nucleus staining	1:1000	Thermo Fisher Scientific	62249	Immunocytochemistry
FITC-488 conjugated dye	Goat anti-rat IgM	1:200	Jackson ImmunoResearch	112095075	Immunocytochemistry, Flow cytometry
Alexa Fluor 555 conjugated dye	Goat anti-mouse	1:500	Thermo Fisher Scientific	A-21422	Immunocytochemistry
Alexa Fluor 555 conjugated dye	Goat anti-rabbit	1:1000	Abcam	ab150086	Immunocytochemistry
CD105-APC	Anti-human	1:11	Miltenyi Biotec	130094926	Flow cytometry
CD90-APC	Anti-human	1:11	Miltenyi Biotec	130095402	Flow cytometry
IgG1-APC	Mouse, isotype	1:11	Miltenyi Biotec	130095902	Flow cytometry
CD44-APC-Vio770	Anti-human	1:11	Miltenyi Biotec	130099149	Flow cytometry
IgG1-APC-Vio770	Mouse, isotype	1:11	Miltenyi Biotec	130096653	Flow cytometry
CD29-PE	Anti-human	1:11	Miltenyi Biotec	130101273	Flow cytometry
IgG1-PE	Mouse, isotype	1:11	Miltenyi Biotec	130095900	Flow cytometry
CD73-PE-Vio770	Anti-human	1:11	Miltenyi Biotec	130104192	Flow cytometry
IgG1-PE-Vio770	Mouse, isotype	1:11	Miltenyi Biotec	130096654	Flow cytometry
CD45-VioBlue	Anti-human	1:11	Miltenyi Biotec	130092880	Flow cytometry
IgG2a-VioBlue	Mouse, isotype	1:11	Miltenyi Biotec	130094671	Flow cytometry

Introduction

Multilineage-differentiating stress-enduring (Muse) cells are a subtype of mesenchymal stromal cells (MSCs) that express stage-specific embryonic antigen 3 (SSEA3). Muse cells can spontaneously differentiate into cells of the endodermal, ectodermal, and mesodermal lineages in vitro, and can be induced to produce cell types from all three lineages and self-renew in vivo without forming teratomas[1–3]. Muse cells migrate to tissues that express sphingosine-1[4], integrate into damaged tissues in vivo when administered intravenously[5,6], differentiate into specific cells needed to repair tissues, and survive over 6 months in animals[7,8]. Muse cells stimulate tissue regeneration and restore functions in many animal models of diseases, e.g., liver diseases[1,3,8–11], stroke[7,12–14], muscle regeneration[1,15,16], skin regeneration[1,3,8,13,17], malignant glioma[18], and myocardial infarction[4,11,19]. No tumors have been reported after in vivo transplantation of Muse cells into animals[5,8,20]. Muse cells also have low telomerase activity and low expression of cell cycle-related genes compared with embryonic stem (ES) and induced pluripotent stem (iPS) cells[1,2,5,10,13,17,19,21,22].

Muse cells have several advantages over other stem cells for regenerative medicine. First, they are pluripotent adult stem cells that can self-renew and differentiate into many other cell types to repair a wide variety of tissues. Second, Muse cells have been isolated from many tissues and are available from autologous and allogeneic sources, including fat, bone marrow, adult blood, umbilical cord blood, and umbilical cord. Third, Muse cells can be readily identified by the combined expression of SSEA3 and a mesenchymal marker, such as CD105, CD29, and CD90[1,5]. Because mesenchymal stromal cells attach to and grow well on plastic, nearly 100% of cells cultured on plastic from Wharton's jelly (WJ) or the cord lining (CL) express mesenchymal markers. Cell culture on plastic effectively purifies a mesenchymal population. Kuroda et al.[21] reported that Muse cells can be sorted and counted from cell cultures grown on plastic based on SSEA3 expression alone. Finally, unlike other pluripotent cells, such as ES or iPS cells, Muse cells do not form teratomas or other tumors. When grown in culture, the self-renewal rate of Muse cells is slower than the production rate of non-Muse differentiated cells, and, therefore, the percentage of Muse cells invariably declines over time in culture.

Many groups have isolated MSCs from the umbilical cord[23–49] and cord blood[23,50–55]. SSEA3+ cells comprise 0.03% to several percent of MSCs cultured from goat skin, human dermal fibroblasts, adipose tissue, and bone marrow[3,20]. Fluorescence-activated cell sorting (FACS) is the most popular method to isolate Muse cells but is inefficient and expensive[3]. Other methods include the use of enzymes and other methods to stress the cells, thereby relying on the stress-resistance of Muse cells to enable cell survival while other cell types die. In mesenchymal cell populations purified by these methods, only 11.6% of cells formed Muse cell clusters[1,3,6].

We describe below a method to efficiently and inexpensively purify and grow large numbers of healthy Muse cells from MSCs isolated from the human umbilical cord (HUC) using magnetic-activated cell sorting (MACS) to isolate

Fig 1. Human umbilical cord (HUC) processing procedure. (A) Bottle for delivering the HUC. (B) Place the HUC in a 10-cm dish. (C) Cut the HUC into smaller 1-cm pieces. (D) Incise the HUC pieces longitudinally. (E) Remove the HUC artery and vein and clean the HUC tissues. (F) Separate Wharton's jelly (WJ, left dish) and cord lining (CL, right dish) tissues. (G) Treat the tissues with collagenase, and seed the cells into cell culture flasks.

SSEA3+ cells[56], expansion in culture, and a second MACS procedure to purify the cell population to >90%. Our method has several advantages. First, the method is gentle and does not damage the cells. We attached the SSEA3 antibody to magnetic beads purchased from Miltenyi Biotec (Bergisch Gladbach, Germany), and these antibody-coated beads bind to SSEA3 on the cell surface and move the cells towards magnets applied to the container walls, allowing SSEA3-negative cells to pass through. Second, the method is very efficient, allowing billions of cells to be sorted in a matter of minutes. Third, the method preserves non-Muse cells, allowing them to flow through for analysis or re-sorting or for use as control cells for comparison with Muse cells. Fourth, CD34+ cells sorted by MACS have been used in clinical trials for some time[57]. Finally, the method yields a relatively high purity (>90%) of SSEA3+ cells. Two previously published studies used MACS to isolate 77.1% and 71.3% Muse cells[14,58].

Materials and Methods

From 6 to 31 January 2017, StemCyte Inc. (Covina, CA, USA) shipped eight HUCs to the W.M. Keck Center for Collaborative Neuroscience, Rutgers, the State University of New Jersey (Piscataway, NJ, USA). Every cord was packed in a bottle filled with the transport medium, which included KH_2PO_4 (0.20 g/L, Sigma-Aldrich P5655, St. Louis, MO, USA), Na_2HPO_4 (anhydrous, 1.15 g/L, Sigma-Aldrich 71640), KCl (0.20 g/L, Sigma-Aldrich 746436), and NaCl (8.00 g/L, Sigma-Aldrich 793566). The bottle was surrounded by ice to maintain it at 4°C. All the cords were collected with patient consent in accordance with the requirements of the Rutgers University Ethics Committee. The shipment from the patient to the laboratory took one day.

HUC MSCs were isolated according to a protocol developed by Yu-Show Fu, as illustrated in Fig 1. Briefly, after removal of blood vessels, the mesenchymal tissue was scraped off from WJ with a scalpel and centrifuged at

Table 2. The Records of the Eight HUCs Showed the Numbers of MSCs and SSEA3+ Cells at Passage 0.

No.	Cord Number / Briefly	Collection Date	Net Weight (g)	Two Groups	HUC-MSCs ($\times 10^6$)	HUC-MSCs/g cord ($\times 10^4$cells/g)	SSEA3+ cells in MSCs (%)	Total SSEA3+ cells ($\times 10^3$)	Total SSEA3+ cells/g cord ($\times 10^3$/g)
1	C-3561762 /62	6 January 2017	21.6	WJ	0.81	3.75	0.40	3.24	0.15
				CL	0.70	3.24	0.30	2.10	0.10
2	C-3561760 /60	10 January 2017	27.5	WJ	1.20	4.36	5.00	60.0	2.18
				CL	0.57	2.07	24.00	136.8	4.97
3	C-3561819 /19	11 January 2017	17.4	WJ[a]	0.70	4.02	11.27	78.89	4.53
4	C-3561843 /43	16 January 2017	37.6	WJ	1.10	2.93	0.01	0.11	0.00
				CL	1.10	2.93	0.19	0.21	0.01
5	C-3561808 /08	19 January 2017	19.4	WJ[a]	0.80	4.12	8.38	67.04	3.46
6	C-3561886 /86	19 January 2017	23.0	WJ	0.85	3.70	3.08	26.18	1.14
				CL	0.50	2.17	10.90	54.5	2.37
7	C-3561896 /96	27 January 2017	47.0	WJ	1.40	2.98	5.93	83.02	1.77
				CL	1.60	3.40	11.61	185.76	3.95
8	C-3561899 /99	30 January 2017	23.8	WJ	0.90	3.78	42.37	381.33	16.02
				CL	1.00	4.20	4.88	48.8	2.05

[a]The MSCs were not successfully derived from CL tissues of No. 19 and 08.

250 x *g* for 5 min at room temperature (RT), and the pellet was washed with serum-free Dulbecco's modified Eagle's medium (DMEM, Gibco, 11330-032, Waltham, MA, USA). Next, the cells were treated with 2 mg/ml collagenase type I solution (Sigma-Aldrich SCR103) for 16 h at 37°C, washed, and treated with 2.5% trypsin (10x) (Thermo Fisher Scientific, 15090046, Waltham, MA, USA) for 30 min at 37°C with agitation. Finally, the cells were washed and cultured in cell culture medium supplemented with 10% fetal bovine serum (FBS, Gibco 10437-028) in a 37°C incubator with 5% CO_2, and the dishes were labeled with the cell passage, name, and date.

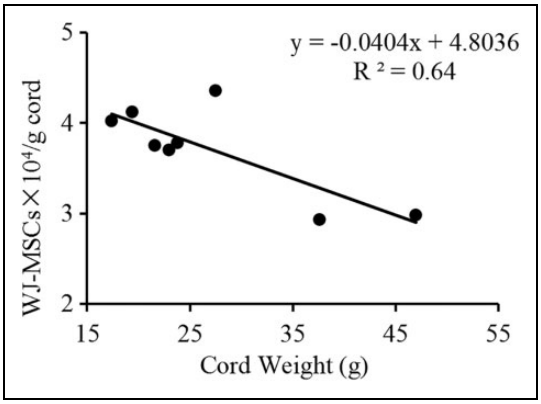

Fig 2. Linear relationship between the number of WJ-MSC cells and cord weight (grams).

Cell Culture and Passage

The first seeding of cells from WJ or CL tissue was named passage 0 (P0), and the next two passages were named P1 and P2. We analyzed the percentage of SSEA3-positive cells in the first three passages. The culture medium contained 10% FBS (Gibco, 10437-028), 2 mM GlutaMAX (Gibco, 35050-061), 1% penicillin-streptomycin (Gibco, 15140-122), 1 ng/mL human basic fibroblast growth factor (bFGF, PeproTech, 100-18B, Rocky Hill, NJ, USA) and DMEM/F12 (Gibco, 11330-032) to 250 mL. We passaged the cells when they reached 90% confluency using TrypLE™ Express (Gibco, 12604-013) to release adherent cells from the cell culture dish.

Immunocytochemistry

The cells were plated at 2×10^4 cells/well in a 24-well plate with a round cover slip (Thermo Fisher Scientific, 1254580) in each well. After plating, the cells were fixed with 4% paraformaldehyde (0.5 mL/well), incubated at RT for 10 min, washed three times with PBS, incubated for 30 min with 5% normal goat serum in PBS without (for surface markers) or with 0.3% Triton X-100 (for Ki-67; Sigma-Aldrich 234729) to block nonspecific antibody binding and incubated with primary antibody overnight at 4°C. The cells were washed three times with PBS and incubated with secondary antibodies for 30 min at RT, and then with Hoechst 33342 nuclear stain (Thermo Fisher Scientific 62249) for 10 min.

Flow Cytometry

The cells ($\sim 0.3 \times 10^6$) were incubated in a 1.5 mL microcentrifuge tube with primary antibodies. For SSEA3, the incubation times were 1 h at 4°C for the primary antibody, and 30 min at 4°C for the secondary antibody. For the other antibodies from Miltenyi Biotec (Bergisch Gladbach, Germany), the incubation time was 10 min. Before loading, we added 2.5 µL of 100 µg/mL propidium iodide solution (Miltenyi Biotec 130093233) to 500 µL of cell suspension

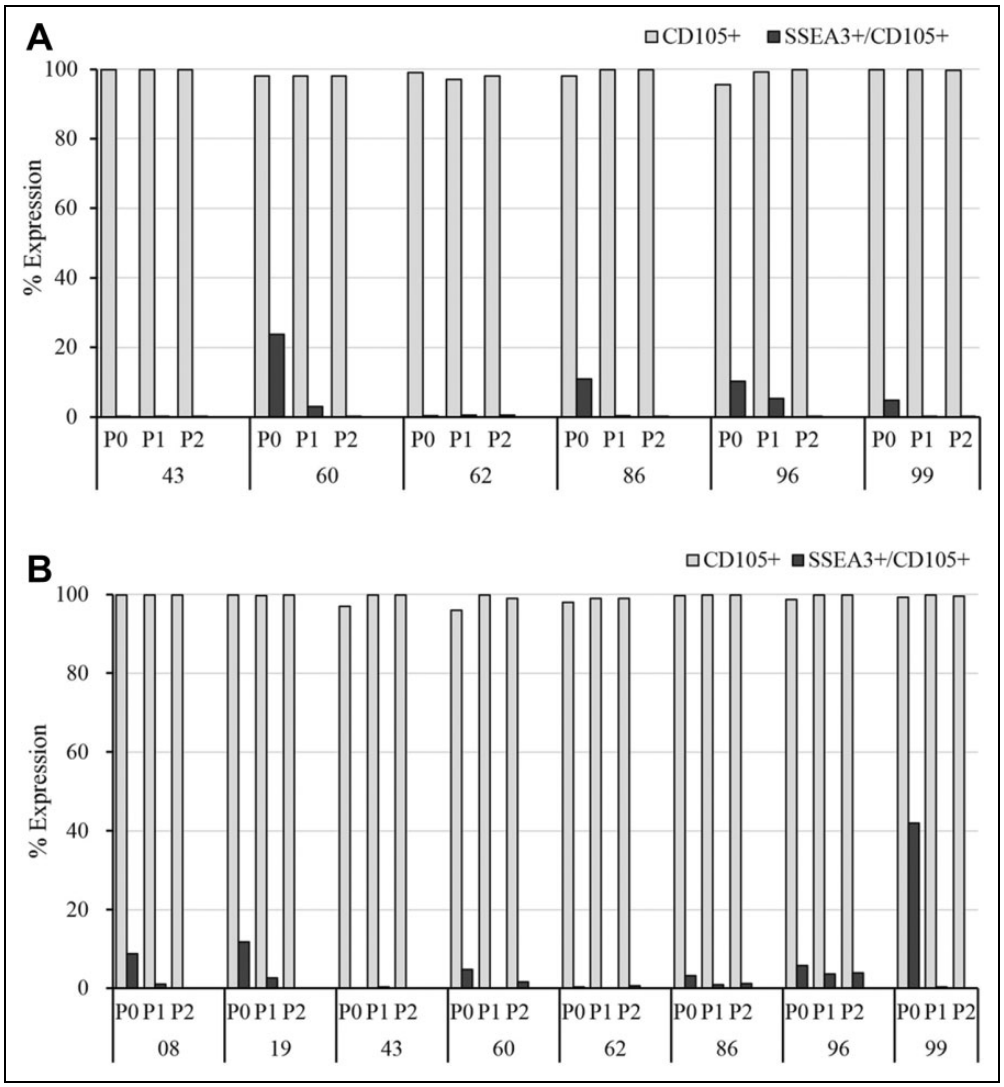

Fig 3. (A) Cord lining (CL) cells. (B) Wharton's jelly (WJ) cells. Gray bars indicate the percent of cells expressing CD105+. Black bars indicate the percent of cells expressing both CD105 and SSEA3. The numbers refer to different samples. P0, P1, and P2 indicate passages 1, 2, and 3, respectively. One-way ANOVA showed that the SSEA3+ percentage dropped sharply between P0 and P1 in the CL group and between P0 and P2 in the WJ group ($P<0.05$).

to label nonviable cells. An isotype control was used in the control group. We used the MACSQuant Analyzer 10 Flow Cytometer (Miltenyi Biotec) equipped with ten fluorescent channels to perform cell sorting and counting and to generate the graphs.

Magnetic-Activated Cell Sorting

Almost all human mesenchymal cells grown on plastic plates express CD105. MACS can be used to positively select for SSEA3+ cells. We loaded $\sim 6 \times 10^6$ cells suspended in 2 mL into a magnetic sorter (MS) column (Miltenyi Biotec 130042201). We added first the SSEA3 antibody and then the anti-rat kappa microbeads (Miltenyi Biotec 130047401) and collected the eluted fraction for analysis on the MACSQuant 10 flow cytometer. The MS column should not be loaded with more than 6×10^6 stained cells suspended in 2 mL. The MS column was washed with 3×1 mL degassed buffer. In the elution step, we pipetted 2 mL of buffer into the MS column, waited 3 min, and then firmly pushed the plunger to expel the magnetically labeled cells. The antibodies used in this study are listed in Table 1.

Doubling Time

To determine the cell doubling time (TD), we plated the cells at a density of 5×10^3 cells/cm^2 and calculated the TD using the following equation (http://www.doubling-time.com):

$$TD = t \times \ln 2 / (\ln Nt - \ln N0),$$

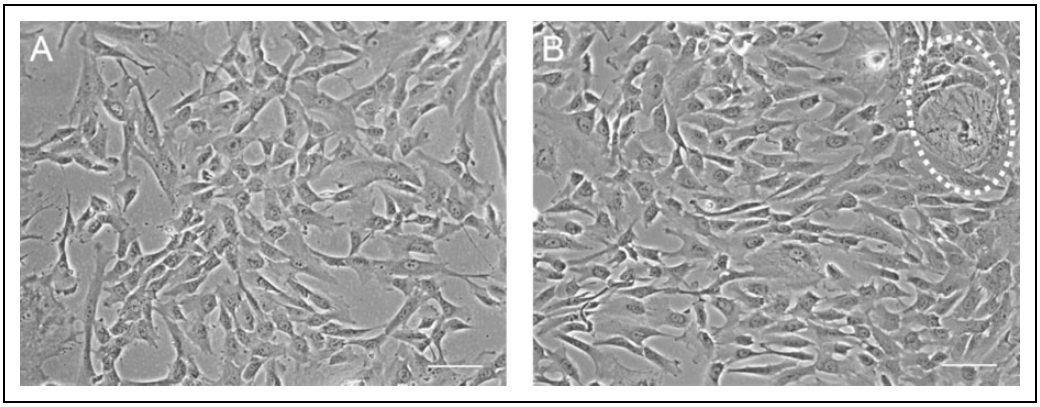

Fig 4. (A) Phase contrast image of Wharton's jelly cells. (B) Phase contrast image of cord lining cells. The tissue was seeded in the dashed and red circles, from which the MSCs grew. Scale bar, 100 μm.

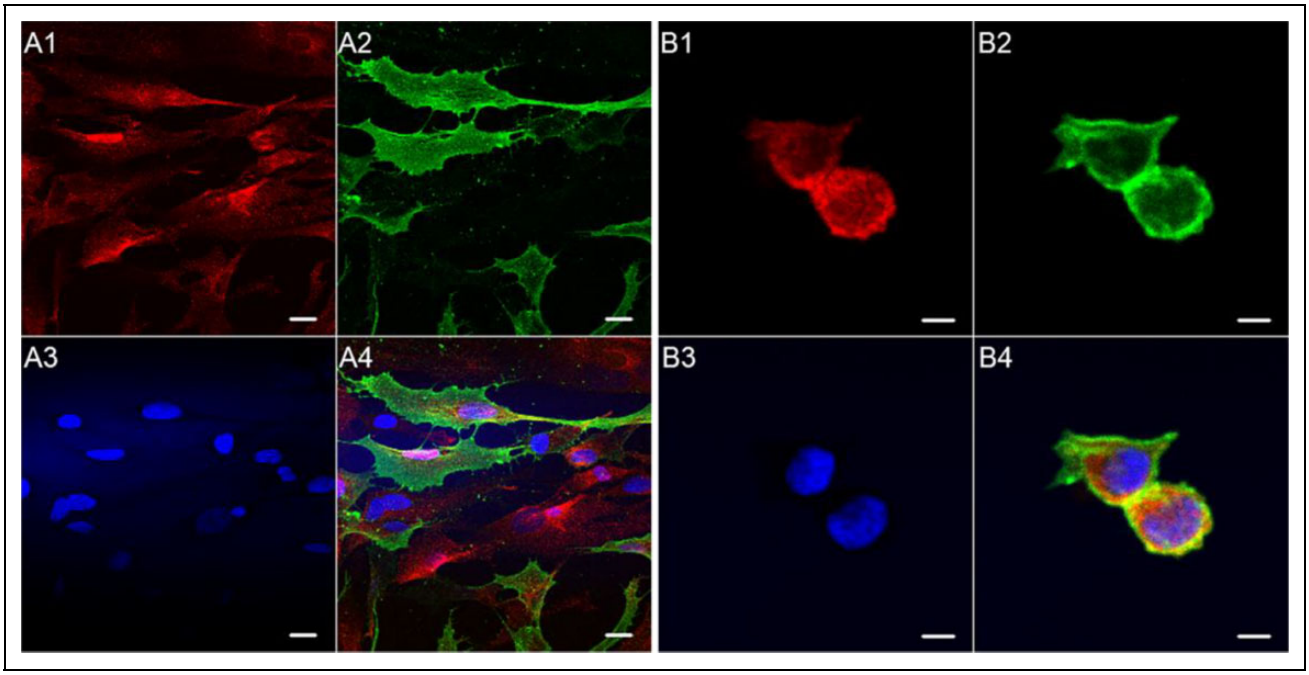

Fig 5. Immunofluorescence images of CD105 (red), SSEA3 (green), and Hoechst 33342 (blue) staining of cultured cells from 96WJP2. (A1) CD105-labeled cells; (A2)some giant SSEA3+ cells with long and very thin processes contacting each other; (A3) nuclei stained with Hoechst 33342.; (A4) merged images. (B) CD105+ and SSEA3+ cells that appear to have just completed dividing. A Zeiss confocal 510 microscope was used to take these pictures at 40X. Scale bar, 20 μm (A) or 5 μm (B).

where N0 is the number of cells inoculated, Nt is the number of cells harvested, and t is the culture time in hours. We calculated the TD of each sample of Muse cells and non-Muse cells.

Statistical Analysis

We used SPSS (IBM, R23.0.0.0, Armonk, NY, USA) to assess differences among groups using one-way analysis of variance (ANOVA). Post hoc analysis of comparisons among groups was performed using the least significant difference (LSD). The results are expressed as the mean ± standard deviation (SD), unless otherwise noted. A probability (*P*-value) of <0.05 was considered significant. We used AxioVision Rel. 4.8.0 SP2 and ZEISS LSM Image Browser (Version 4.2.0.121, Zeiss, Wetzlar, Germany) to obtain pictures.

Results

Both WJ and the CL of HUCs yielded large numbers of MSCs. Table 2 shows the number of MSCs and SSEA3+

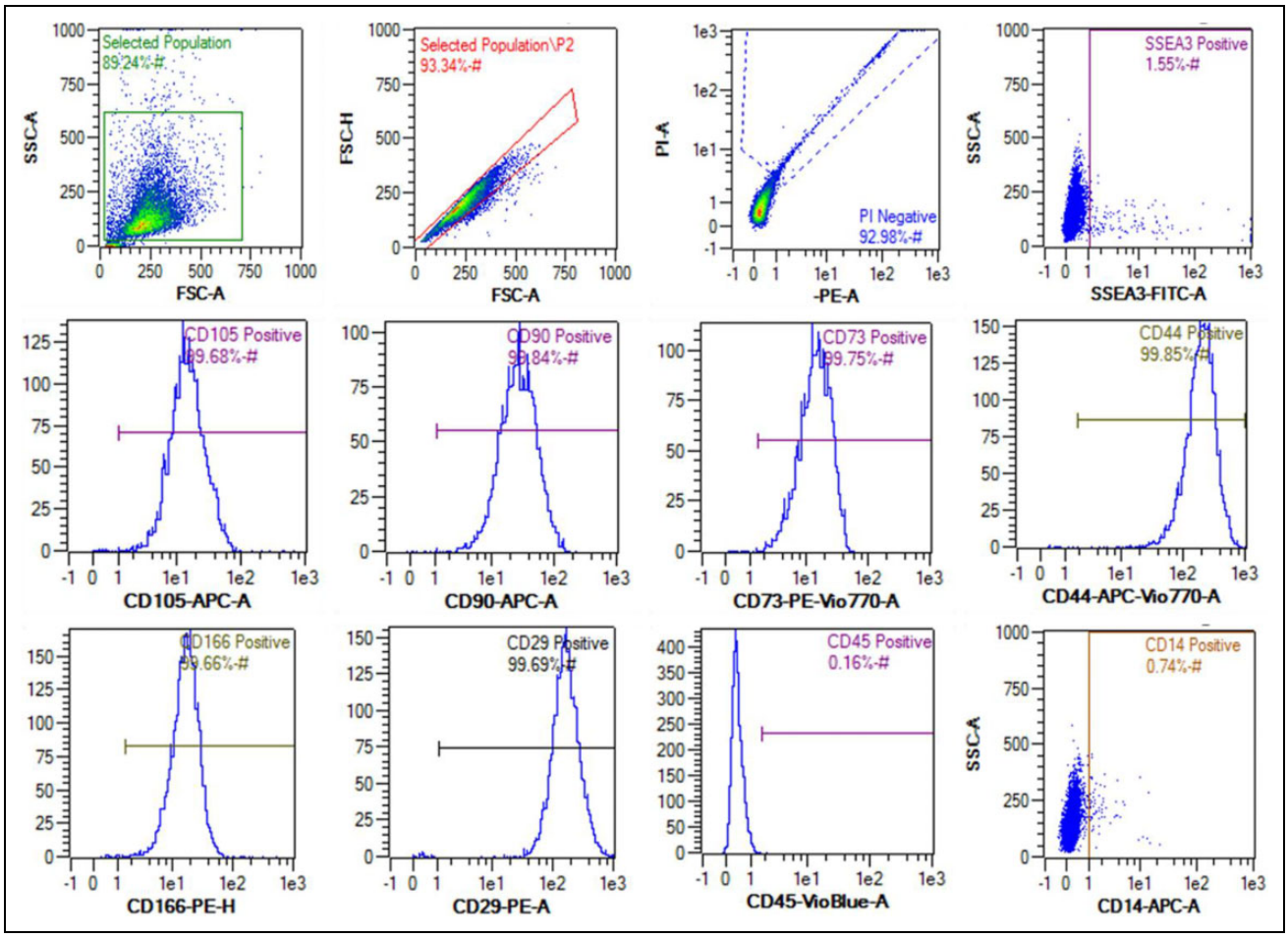

Fig 6. Flow cytometry analysis of HUC-derived MSCs from 96WJP2. We used SSC-A and FSC-A to gate cells from debris and FSC-H and FSC-A to gate single cells from cell clusters. Then, PI staining was used to exclude dead cells. The results showed that 92.98% of the total cell population was alive and in a single-cell suspension, 1.55% was SSEA3+, and over 99% was CD105+, CD90+, CD73+, CD44+, CD166+, CD29+, CD14– and CD45–.

Table 3. MACS Performances from 96WJP2 to 96WJP10.

Passage	Total alive cells before MACS($\times 10^6$)	Percentage of Muse cells before MACS (%)	Number of Muse cells before MACS ($\times 10^5$)	Number of sorted cells($\times 10^5$)	Percentage of Muse cells in sorted population (%)	Number of sorted Muse cells (10^5)	Sorting rate (%)[a]
96WJP2	5.24	28.27	14.81	3.60	93.84	3.38	22.80
96WJP3	6.00	14.80	8.88	9.00	92.94	8.36	94.19
96WJP3	6.00	14.80	8.88	9.10	92.94	8.46	95.24
96WJP4	5.00	48.64	24.32	7.50	92.56	6.94	28.54
96WJP4	5.20	41.12	21.38	8.00	89.85	7.19	33.61
96WJP5	6.00	59.42	35.65	9.40	88.35	8.30	23.29
96WJP5	4.50	40.45	18.20	6.00	93.36	5.60	30.77
96WJP6	6.00	43.95	26.37	10.00	96.29	9.63	36.51
96WJP7	5.70	47.87	27.28	7.70	94.45	7.27	26.65
96WJP8	6.00	28.10	16.86	4.50	91.02	4.10	24.29
96WJP8	6.00	28.10	16.86	3.60	91.02	3.28	19.43
96WJP9	6.20	25.66	15.90	5.00	84.22	4.21	26.46
96WJP10	2.60	25.98	6.75	3.00	87.91	2.64	39.04

[a]Sorting rate (%) =Number of sorted Muse cells/Number of Muse cells before MACS $\times$100%

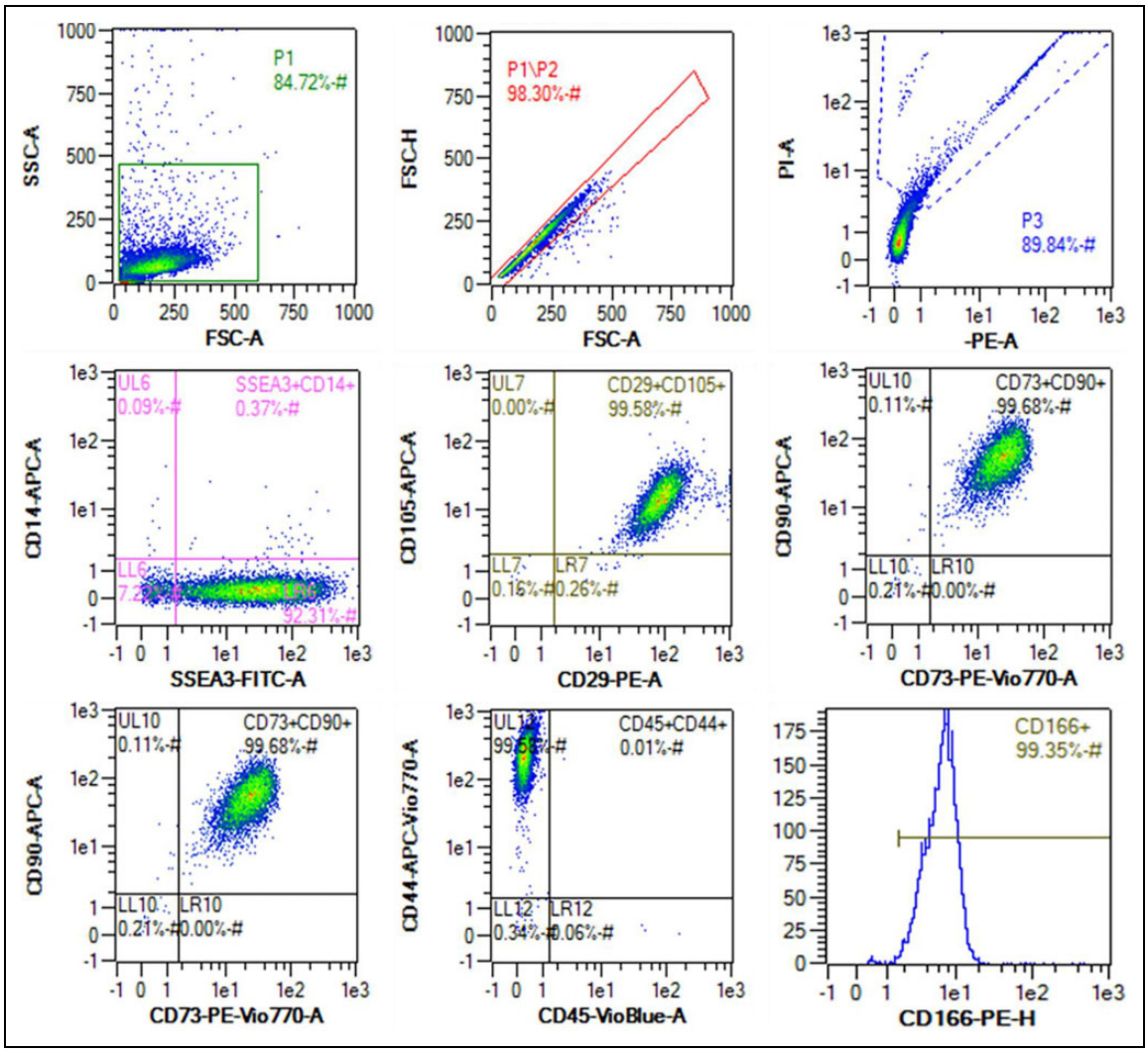

Fig 7. Flow cytometry results of SSEA3+ cells from 96WJP2 subjected to MACS. The sample was analyzed immediately after sorting. In total, 89.84% of all cells were alive and in a single-cell suspension. Of the sorted population, 92.31% were SSEA3+, while the other 7.27% appeared to be debris according to the diameter. Over 99.5% of the population was CD105+, CD29+, CD90+, CD73+, CD44+, CD166+, CD14– and CD45–.

cells at P0. The average concentrations of MSCs and SSEA3+ cells per gram of tissue were $(3.70 \pm 0.55)\times10^4$ WJ-MSCs, $(1.89 \pm 1.67)\times10^3$ WJ-SSEA3+ cells, $(3.00 \pm 0.80) \times 10^4$ CL-MSCs, and $(2.24 \pm 2.00)\times10^3$ CL-SSEA3+ cells. Heavier cords had more WJ-MSCs ($R^2 = 0.64$, $P = 0.01 < 0.05$, Fig 2). The 99WJ group had an unusually high percentage of SSEA3+ cells at P0 (42.37%). However, cord weight did not correlate with the percentage of CL-MSCs, WJ-SSEA3+ cells, or CL-SSEA3+ cells. The number of WJ-MSCs did not correlate with that of CL-MSCs or WJ-SSEA3+ cells, nor was there a correlation between the number of CL-MSCs and that of CL-SSEA3+ cells.

We cultured WJ and CL cells separately and compared the SSEA3+ percentage over multiple passages (Fig 3). In the P0 group, more than 98% of all cells from both WJ and the CL were CD105 positive, and this percentage was even higher in the P1 and P2 groups. At P0, the percentages of SSEA3+ cells were $4.97\% \pm 4.30\%$ and $5.26\% \pm 5.14\%$ in WJ and the CL, respectively. However, the SSEA3+ percentage dropped sharply between P0 and P2 in the CL group and between P0 and P1 in the WJ group.

The WJ-MSCs and CL-MSCs had similar morphology (Fig 4); they were spindle-shaped or triangular with a large oval nucleus in the center of the cell body and one or several nucleoli. As shown in Fig 4B, the tissue was seeded in the red circle, from which the MSCs grew. Fig 5A1 shows that all cells were CD105 positive, and Fig 5A2 shows that the SSEA3+ cells often had long, thin processes and tried to make connections with surrounding cells. The flat cell bodies had an irregular shape but could be as large as 30×100 μm. Fig 5A3 shows large oval nuclei of up to 20 μm in diameter. Fig 5B shows that dividing cells had smaller and

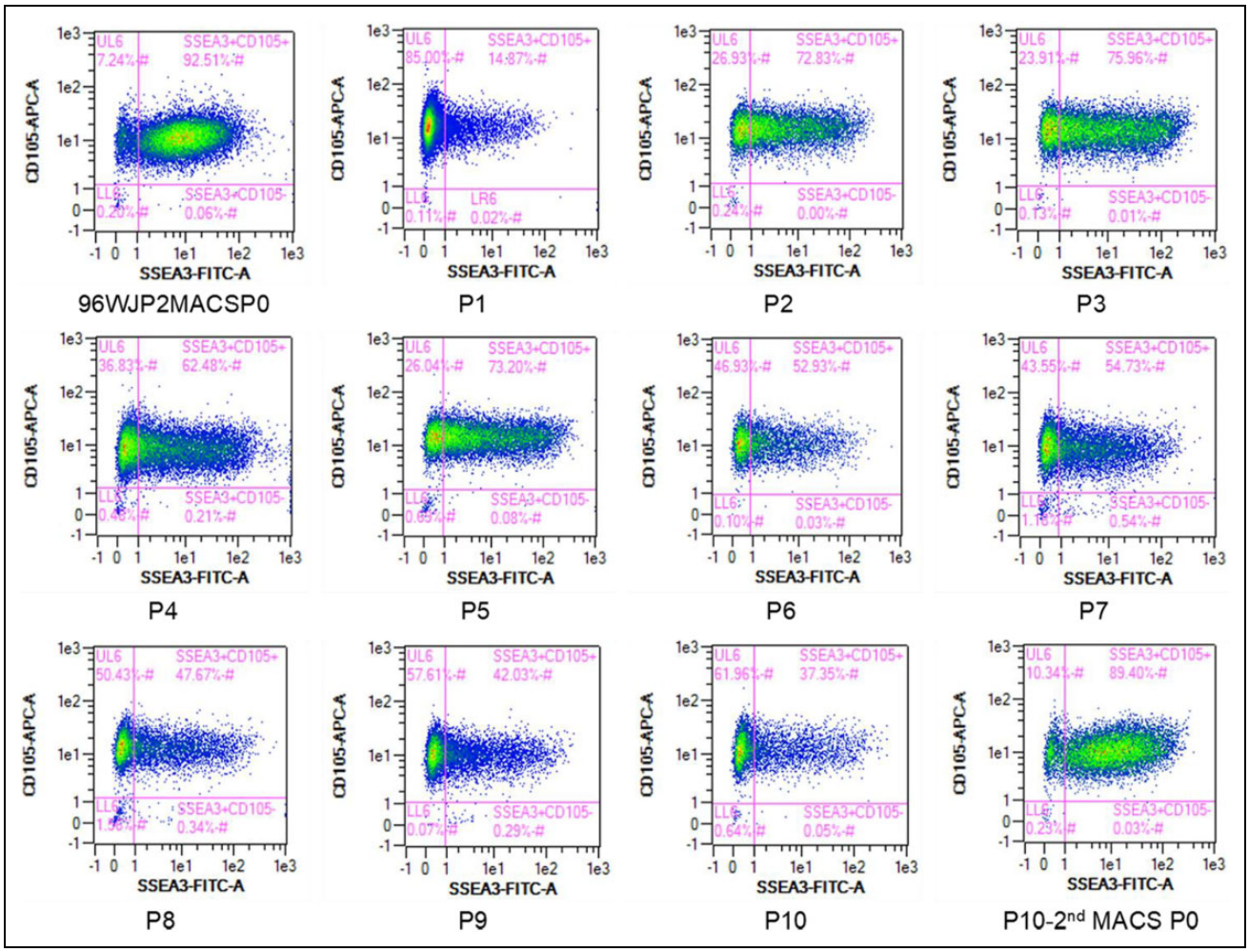

Fig 8. Change in percentage of SSEA3+ cells after MACS in the following ten passages. 96WJ-P2-MACS-P0 indicates the cell population immediately after magnetic sorting, and 93.77% of the total population was SSEA3+ but CD14–. The other 6.19% appeared to be debris according to the diameter. Then, the sorted cells were cultured, and cells of the next passage were collected every 4 days. The SSEA3+ percentage decreased to 14.8% in the first passage but ranged from 62.5% to 75.9% between P2 and P5 before declining to 42.0%–54.7% between P6 and P9. At P10, the cultures still contained 37.3% SSEA3+ cells. After P10, we resorted the cells and achieved 89.4% SSEA3+ cells. In all passages, the CD105+ percentage remained over 99.0%.

rounder cell bodies but maintained their typical membrane SSEA3+ staining. Both WJ- and CL-derived MSCs were CD105+, CD90+, CD73+, CD44+, CD166+, CD29+, CD45– and CD14– (Fig 6).

We cultured frozen 96WJP2 cells, which showed an increase in SSEA3+ cell percentage from 3.91% to 28.27%. Another culture of frozen 96WJP2 cells had 20.62% SSEA3+ cells, confirming this phenomenon of an increased percentage after freezing. Thus, the freezing process (severe environment) may induce higher Muse cell percentages. Cells in each passage from 96WJP2 to 96WJP10 were subjected to MACS.

We used MACS to sort $(1.23 \pm 0.38) \times 10^5$ cells from 1 million MSCs (Table 3). Of the sorted population, 91.44%±3.22% were SSEA3+ cells, demonstrating the efficiency of this method. For 96WJP3, the sorting rates were 94.19% and 95.24%, and the average rate for the other groups was 28.31% ± 6.11%, indicating that approximately 28.31% of all SSEA3+ cells were sorted from the MSC population. Further analysis by flow cytometry showed that the sorted population expressed SSEA3 more strongly than the nonsorted population. In 96WJP8, the percentage of SSEA3+ cells in the MSC population dropped to 28.10%, suggesting that previous passages should be used. Further analysis showed that the sorted cells were SSEA3+, CD105+, CD90+, CD29+, CD44+, CD73+, CD166+, CD14–, and CD45– (Fig 7).

We also monitored the SSEA3+ cell percentage in MACS-sorted 96WJP2 cells over 10 passages (Fig 8). Immediately after MACS, 93.8% of the cells were SSEA3+. In the first passage after MACS, the percentage of SSEA3+ cells decreased to 14.8%, but the SSEA3+ cell population

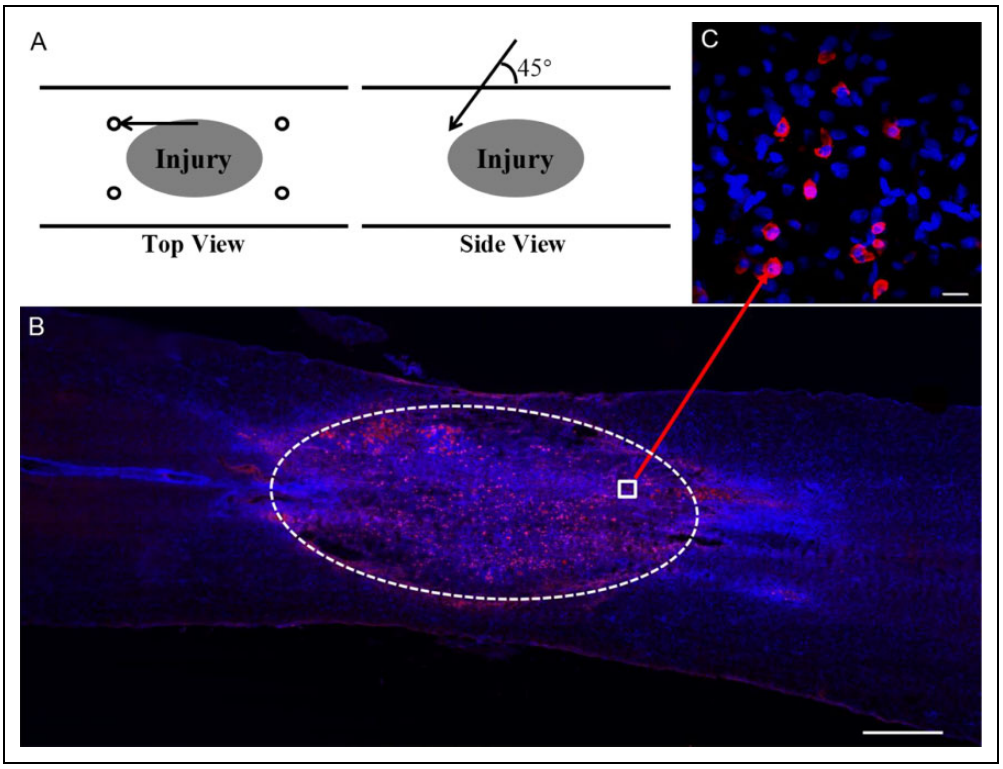

Fig 9. (A) The diagram on top left indicates the injection sites from the dorsal surface and the side view. (B) A horizontal section of the spinal cord at 4 weeks after transplantation of SSEA3+ HUC cells into dorsal entry zones of the spinal cord above and below the injury site. The sections were stained with STEM101 (anti-human nuclear protein, red) and Hoechst 33342 (blue). Scale bar, 500 μm. The dashed circle indicates the injury site. (C) An image obtained under a Zeiss confocal 510 microscope at 40X showing the HUC cells. Scale bar, 10 μm.

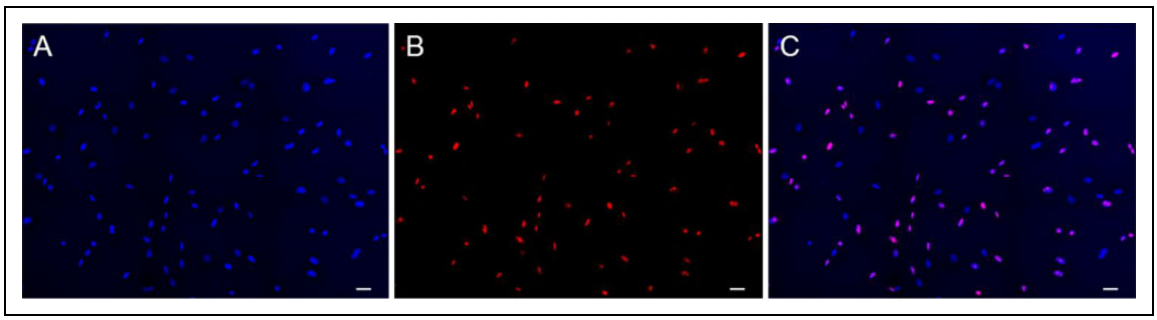

Fig 10. Ki-67 staining of 96CLP1 cells. (A) Hoechst, (B) Ki-67, (C) Merge. Ki-67 is a nuclear protein and marker of proliferating cells. Approximately 65% of all cells were Ki-67+, indicating that population was actively proliferating. Scale bar, 50 μm.

rebounded, and the cultures maintained 62.48%–75.96% SSEA3+ cells from P2 to P5. The percentage decreased to 42.03%–54.73% from P6 to P9, and the P10 culture had 37.35% SSEA3+ cells. After P10, we resorted the cells and achieved 89.40% SSEA3+ cells. The MACS-culture-MACS process can yield many millions of Muse cells.

Finally, we transplanted HUC-derived SSEA3+ and CD105+ cells into the spinal cord of two adult Sprague-Dawley rats at 2 weeks after spinal cord injury (SCI) with a 12.5-mm T11 weight drop contusion. Muse cells (4×10^5) were injected into the dorsal root entry zone of the spinal cord at four points an equal distance above and below the injury site. As shown in Fig 9, the cells survived for 4 weeks after transplantation in rats that were not immunosuppressed. The transplanted cells were stained with an antibody for the human nucleus (STEM101+) but were otherwise negative for Nestin, GFAP, NeuN, NF155, and Iba1. The immune tolerance of the rat for these cells and the long-term survival of the cells transplanted into the spinal cord are characteristics of Muse cells transplanted into brain[13,14].

Table 4. Doubling Times for the First Three Passages of WJ and CL Cells (Hours).

Passages	TD of non-Muse cells (hrs)	TD of Muse cells (hrs)	Passages	TD of non-Muse cells (h)	TD of Muse cells (h)
60CLP1	30.1	–592.4[a]	60CLP2	54.8	–25.5[a]
62CLP1	48.6	41.5	62CLP2	48.0	45.7
43CLP1	42.5	239.3	43CLP2	54.0	86.4
99CLP1	37.6	–47.5[a]	99CLP2	48.0	40.2
mean	39.7	NA	mean	51.2	NA
SD	7.8	NA	SD	3.7	NA
60WJP1	61.8	–31.6	60WJP2	50.6	11.5
62WJP1	51.0	–156.6[a]	62WJP2	41.5	14.0
86WJP1	50.5	108.4	86WJP2	61.5	56.1
96WJP1	44.1	52.9	08WJP2	90.4	–71.7[a]
99WJP1	44.5	–78.8[a]	19WJP2	67.5	–54.9[a]
mean	50.4	NA	Mean	62.3	NA
SD	7.2	NA	SD	18.6	NA

[a]Minus numbers indicate that the cells did not divide at all.

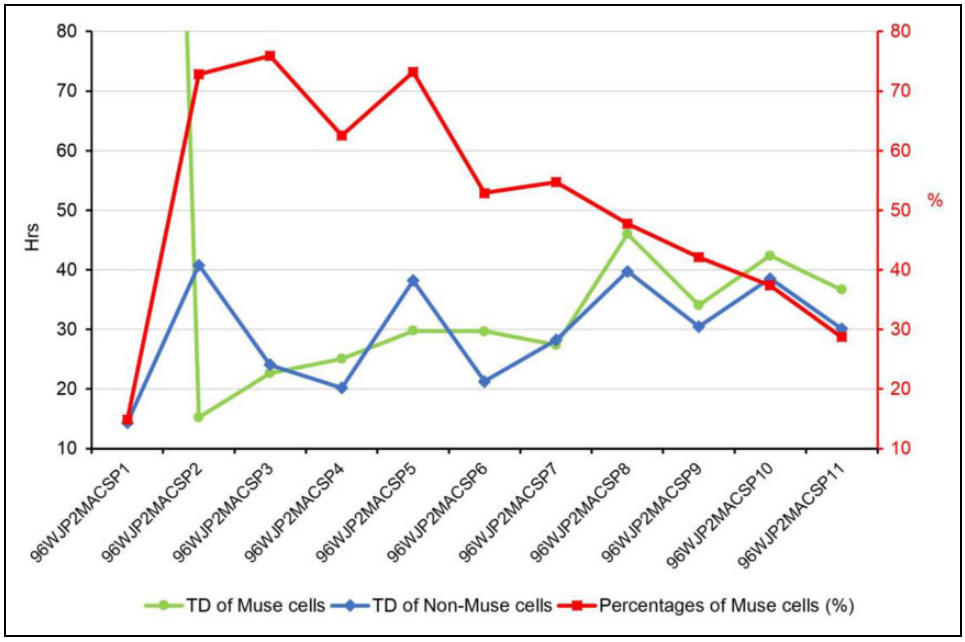

Fig 11. Doubling time (TD) of Muse and non-Muse cells at P1 to P10 after MACS. The left axis indicates hours for the doubling of Muse cells (green) and non-Muse cells (blue). The right axis (red) indicates the percent of Muse cells (red). The TD in P1 was 403 h for Muse cells, indicating that they were barely proliferating, and 14.4 h for non-Muse cells. The TD of Muse cells was 24.9 $\pm$ 5.4 h from P2 to P7, indicating that the number of Muse cells doubled approximately every day, and increased to 39.8 $\pm$ 5.4 h from P8 to P11. For non-Muse cells, the TD was rather stable at 31.2 $\pm$ 7.8 h from P2 to P11. Considering the percentage of Muse cells in the total population, P2 to P7 were the best passages to be resorted to acquire millions of Muse cells.

Discussion

Our results showed the presence of numerous SSEA3+ and CD105+ double-positive cells in both WJ and CL tissues. SSEA3 is a pluripotent cell surface marker. According to Dezawa[3], SSEA3+ and CD105+ cells are likely to be Muse cells. However, the percentage of SSEA3+ cells quickly decreased after 2–3 passages, suggesting that non-Muse (i.e., SSEA3-) cells divide faster than SSEA3+ cells. Approximately 65% of the MSCs (CD105+) were positive for Ki-67 (see Fig 10).

The TD is shown in Table 4 for some cell populations in the first three passages. The TD of non-Muse cells was stable, and statistical analysis showed no significant difference between CLP1 and CLP2 ($P = 0.18$) or between WJP1 and WJP2 ($P = 0.12$). Most SSEA3+ cells remained in G0 in the absence of stimulatory factors. The negative numbers in Table 4 indicate that the cells did not divide at all. In the MACS-sorted SSEA3+ cell populations (Fig 11), the TD averaged 30.9 $\pm$ 9.2 h, nearly the same as that of human fibroblasts. The TD increased with more passages, while the

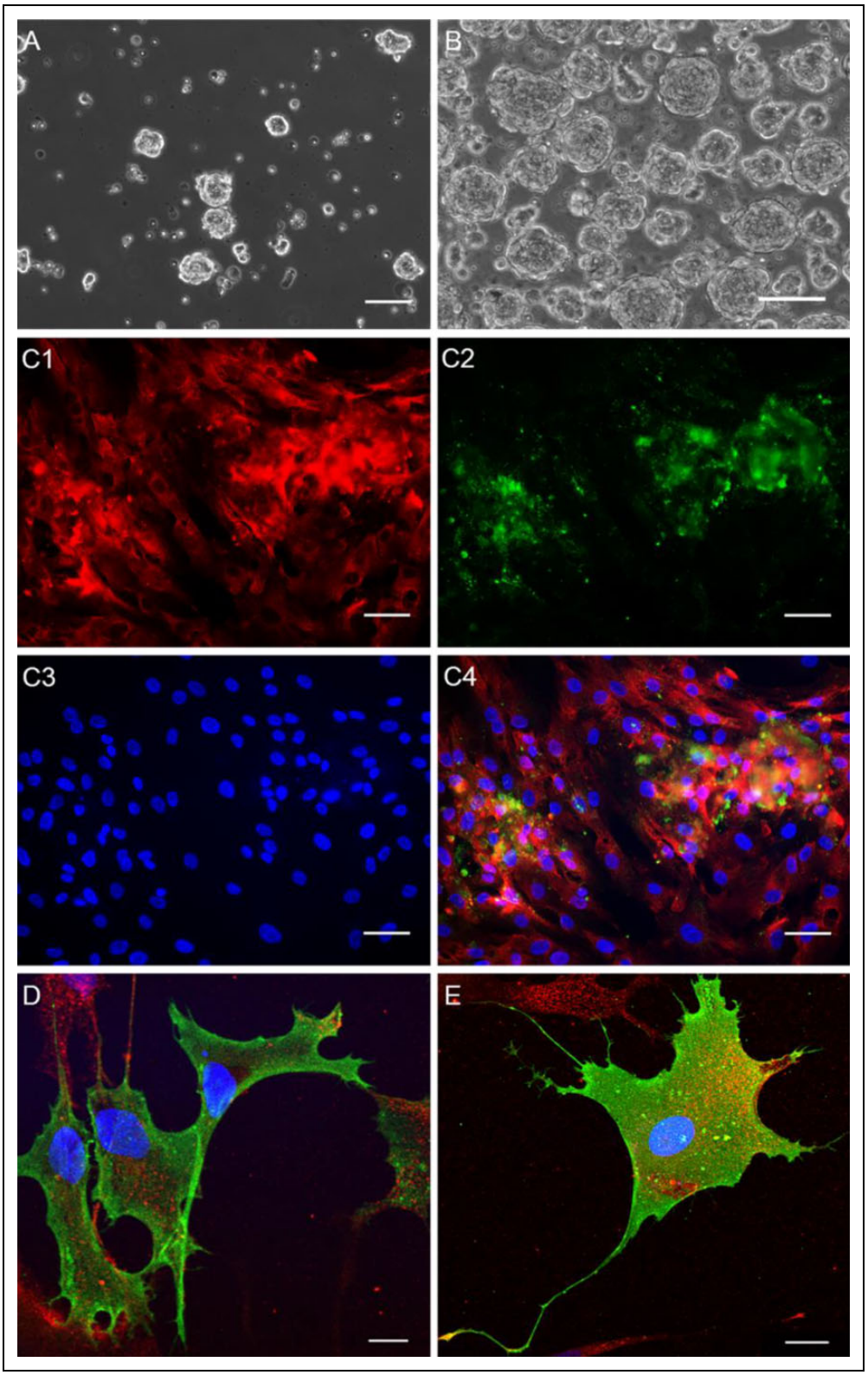

Fig 12. Muse cell clusters on polyHEMA-coated dishes. (A) On day 2 after seeding the cells, clusters had formed but were no more than 50 μm in diameter. (B) On day 7, many clusters had formed with a diameter of approximately 100 μm. (C) Immunocytochemistry of the clusters that were transferred onto coverslips and cultured for 8 h. (C1) CD105 (red), (C2) SSEA3 (green), (C3) Hoechst 33342 (blue), (C4) Merge. Almost all the cells were CD105+, and approximately half were SSEA3+. (D, E) Two images obtained under a Zeiss confocal 510 microscope at 40X showing the sorted Muse cells after culture for 2 days. Scale bars: 50 μm (A, C), 100 μm (B), 10 μm (D), and 20 μm (E).

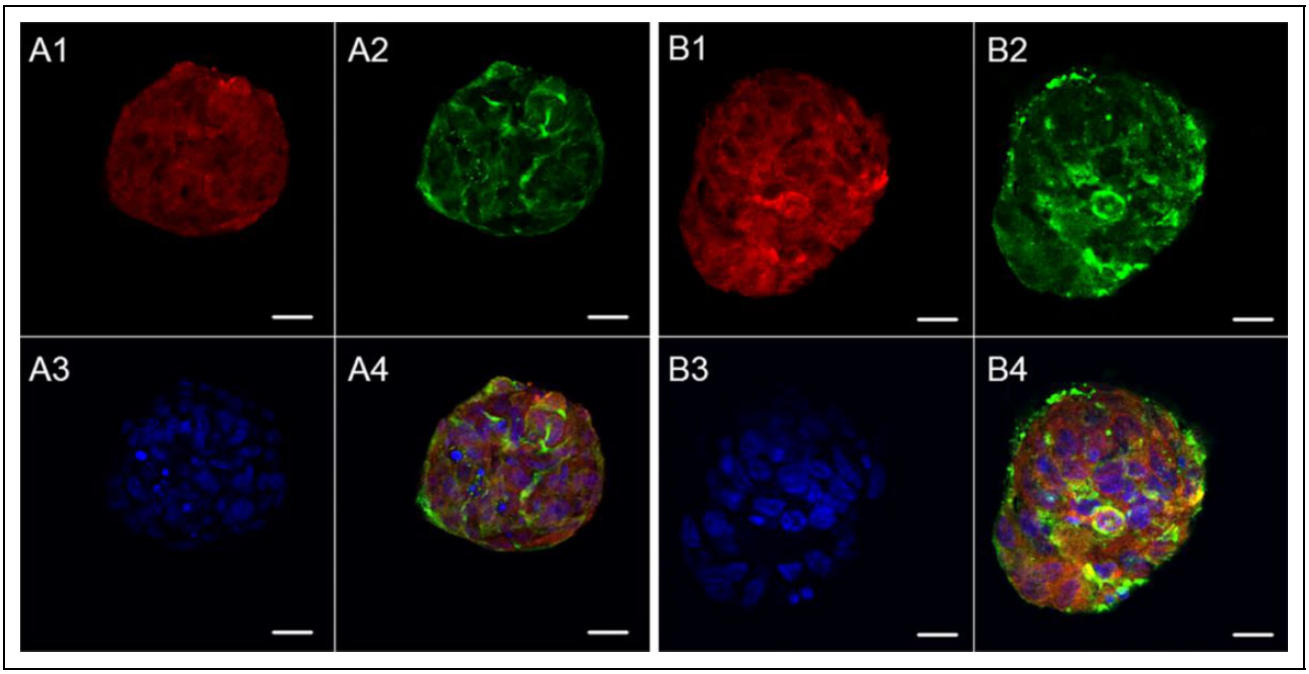

Fig 13. Expression of neural and glial markers in embryoid bodies cultured on polyHEMA-coated dishes for 7 days in induction medium. The sample was from 96WJ-P2-MACS-P0, and the cells formed neural spheres with a diameter of 60–100 μm after 7 days of induction. The left four images show NeuN (A1), Nestin (A2), Hoechst 33342 (A3), and merge (A4). The right four images show GFAP (B1), NF-155 (B2), Hoechst 33342 (B3), and merge (B4). Scale bar, 20 μm.

percentage of SSEA3+ cells decreased. Fig 11 shows that after the first round of MACS, cells in P2–P7 appear to be the best for re-sorting for transplant experiments.

In this study, MACS using MS columns efficiently isolated SSEA3+ cells from WJ and CL tissues. Before sorting, <5% of the cells were SSEA3+, but after MACS, 91.44% ± 3.22% of the cells were SSEA3+. Only Muse cells with strong SSEA3 expression (~28.31%) were isolated. Our experience suggests two guidelines for the sorting procedure: (1) Do not load the column with more than 6 million cells, and load the cell suspension in a 2 mL volume rather than the suggested 0.5 mL to avoid the cells sticking to the column. (2) In the elution step, pipette 2 mL rather than 1 mL of the buffer onto the column, and wait 3 min before applying the plunger.

As shown in Fig 5, individual SSEA3+ cells showed typical membrane staining, while previous studies showed only cell clusters with SSEA3 staining. While the average size range of most human cells is 2–120 μm, SSEA3+ cell bodies are 25–90 μm, similar to the size of macrophages (20–80 μm), and the nucleus is approximately 20 μm. Some Muse cells had very large cell bodies, up to 110 μm in length. In contrast to non-Muse cells, Muse cells have many long processes that extend towards surrounding cells. Dividing SSEA3+ cells have round and much smaller cell bodies of 10 μm, while the nucleus is ~7 μm.

MACS-sorted SSEA3+ cells cultured on polyHEMA-coated dishes formed small SSEA3+ cell clusters on day 2 after plating (Fig 12) and many large clusters 7 days later. We isolated these clusters and cultured them in non-polyHEMA-coated wells for 8 h; the cell clusters attached to the plate and stained SSEA3+ (Fig 12). One study[59] suggested adding Triton X-100 to the blocking solution for immunohistological staining of Muse cells, but our samples showed no SSEA3 signal after treatment with 0.3% Triton X-100. Triton X-100 is a detergent that permeabilizes lipid membranes, so the results confirm that SSEA3 is expressed on the cell surface.

We also cultured the sorted Muse cells in a neural precursor cell culture medium: 2% B-27 supplement (Thermo Fisher Scientific 17504-044), 2 mM GlutaMAX (Thermo Fisher Scientific 35050-061), 30 ng/mL bFGF (PeproTech 100-18B, Rocky Hill, NJ, USA), 30 ng/mL EGF (PeproTech AF-100-15), 1% penicillin-streptomycin (Thermo Fisher Scientific 15140122) and Neurobasal medium (Gibco 21103049). It took 7 days to induce differentiation into neural precursor cells that formed specific spheres positive for Nestin, NeuN, GFAP and NF-155 (see Fig 13), indicating that the induction was successful and that the neural precursor cells were multipotent.

SSEA3 expression on the transplanted cells could not be determined because rats are the host species of the SSEA3 antibody. This pilot experiment, however, clearly showed that Muse cells were not immune rejected in the first 4 weeks. Other studies have shown that human Muse cells survive transplantation and are not immune rejected in

FSGS-BALB/c mice at 5 weeks[22]. Once the Muse cells differentiate into other cell types, they apparently do not survive without immunosuppression[21]. Muse cells have immunomodulatory effects[60]. A similar phenomenon was reported in a study of MSCs in a rat myocardial infarction model, in which the MHC profile changed, and the immunomodulatory function of allogeneic MSCs was lost upon differentiation into myocardial cells[61]. Immunosuppressants may be required for longer survival of Muse cell progeny. Migration appears to be guided by S1P–S1PR2[18], which mediates the homing of Muse cells into the damaged heart for long-term tissue repair and functional recovery after acute myocardial infarction.

Our finding that HUC-derived SSEA3+ and CD105+ cells survive and migrate after transplantation into an injured rat spinal cord without immune suppression reaffirms the findings of Uchida et al.[13,14], who found that Muse cells survived long term when transplanted into the rat brain after stroke. We identified HUC SSEA3/CD105 cells by the antibody STEM101® (Takara, Shiga, Japan) against a human nuclear protein. This antibody does not recognize mouse, rat, or nonhuman primate cells. SSEA3+/CD105+ cell survival in an injured rat spinal cord without immunosuppression is consistent with the immune tolerance of human Muse cells, which express HLA-G[22,62]. Although HUC-derived SSEA3+ and CD105+ cells form neural spheres (ectodermal), we did not observe induction into endodermal or mesodermal cells. However, past studies have shown that HUC-derived SSEA3+ and CD105+ cells can differentiate into the three lineages[63–67].

Conclusion

We believe that we have developed an efficient method of isolating, growing, and purifying SSEA3+ and CD105+ cells from HUCs using MACS.

Acknowledgments

The authors would like to express their appreciation to Sean P O'Leary for animal care, tissue fixation and other technical support.

Author Contributions

Conceptualization, Zikuan Leng; investigation, Dongming Sun; methodology, Zikuan Leng, Zihao Huang, Ning Chiang, Nikhit Kethidi, Ahmed Sabra and Yoshihiro Kushida; resources, Iman Tadmori; writing of original draft, Zikuan Leng; manuscript review and editing, Dongming Sun and Wise Young; supervision, Xijing He and Wise Young; funders, Xijing He and Wise Young; co-corresponding authors, Xijing He and Wise Young.

Ethics Approval

This study was approved by Rutgers University Ethics Committee.

Statement of Human and Animal Rights

All of the experimental procedures of this study were conducted in accordance with protocols approved by Rutgers University Institutional Animal Care and Use Committee.

Statement of Informed Consent

There were no human subjects in this research, and informed consent was not applicable.

Declaration of Conflicting Interests

The author(s) declared no potential conflicts of interest with respect to the research, authorship, and/or publication of this article.

Funding

The author(s) disclosed receipt of the following financial support for the research and/or authorship of this article: This work was supported by the China Scholarship Council (CSC, No. 201506280109) and the Natural Science Foundation of China (No. 81571209).

References

1. Kuroda Y, Kitada M, Wakao S, Nishikawa K, Tanimura Y, Makinoshima H, Goda M, Akashi H, Inutsuka A, Niwa A, Shigemoto T, Nabeshima Y, Nakahata T, Nabeshima Y, Fujiyoshi Y, Dezawa M. Unique multipotent cells in adult human mesenchymal cell populations. Proc Natl Acad Sci USA. 2010;107(19):8639–8643.
2. Wakao S, Kitada M, Kuroda Y, Shigemoto T, Matsuse D, Akashi H, Tanimura Y, Tsuchiyama K, Kikuchi T, Goda M, Nakahata T, Fujiyoshi Y, Dezawa M. Multilineage-differentiating stress-enduring (Muse) cells are a primary source of induced pluripotent stem cells in human fibroblasts. Proc Natl Acad Sci USA. 2011;108(24):9875–9880.
3. Dezawa M. Muse cells provide the pluripotency of mesenchymal stem cells: direct contribution of Muse cells to tissue regeneration. Cell Transplant. 2016;25(5):849–861.
4. Tanaka T, Nishigaki K, Minatoguchi S, Nawa T, Yamada Y, Kanamori H, Mikami A, Ushikoshi H, Kawasaki M, Dezawa M, Minatoguchi S. Mobilized Muse cells after acute myocardial infarction predict cardiac function and remodeling in the chronic phase. Circ J. 2018;82(2):561–571.
5. Ogura F, Wakao S, Kuroda Y, Tsuchiyama K, Bagheri M, Heneidi S, Chazenbalk G, Aiba S, Dezawa M. Human adipose tissue possesses a unique population of pluripotent stem cells with nontumorigenic and low telomerase activities: potential implications in regenerative medicine. Stem Cells Dev. 2014; 23(7):717–728.
6. Heneidi S, Simerman AA, Keller E, Singh P, Li X, Dumesic DA, Chazenbalk G. Awakened by cellular stress: isolation and characterization of a novel population of pluripotent stem cells derived from human adipose tissue. Plos One. 2013;8(6): e64752.
7. Yamauchi T, Kuroda Y, Morita T, Shichinohe H, Houkin K, Dezawa M, Kuroda S. Therapeutic effects of human multilineage-differentiating stress enduring (Muse) cell transplantation into infarct brain of mice. Plos One. 2015;10(3): e0116009.
8. Iseki M, Kushida Y, Wakao S, Akimoto T, Mizuma M, Motoi F, Asada R, Shimizu S, Unno M, Chazenbalk G, Dezawa M. Muse Cells, nontumorigenic pluripotent-like stem cells, have liver regeneration capacity through specific homing and cell

replacement in a mouse model of liver fibrosis. Cell Transplant. 2017;26(5):821–840.
9. Katagiri H, Kushida Y, Nojima M, Kuroda Y, Wakao S, Ishida K, Endo F, Kume K, Takahara T, Nitta H, Tsuda H, Dezawa M, Nishizuka SS. A distinct subpopulation of bone marrow mesenchymal stem cells, Muse cells, directly commit to the replacement of liver components. Am J Transplant. 2016; 16(2):468–483.
10. Wakao S, Kitada M, Kuroda Y, Dezawa M. Isolation of adult human pluripotent stem cells from mesenchymal cell populations and their application to liver damages. Methods Mol Biol. 2012; 826:89–102.
11. Kuroda Y, Kitada M, Wakao S, Dezawa M. Bone marrow mesenchymal cells: how do they contribute to tissue repair and are they really stem cells? Arch Immunol Ther Exp (Warsz). 2011;59(5):369–378.
12. Xu H, Miki K, Ishibashi S, Inoue J, Sun L, Endo S, Sekiya I, Muneta T, Inazawa J, Dezawa M, Mizusawa H. Transplantation of neuronal cells induced from human mesenchymal stem cells improves neurological functions after stroke without cell fusion. J Neurosci Res. 2010;88(16):3598–3609.
13. Uchida H, Morita T, Niizuma K, Kushida Y, Kuroda Y, Wakao S, Sakata H, Matsuzaka Y, Mushiake H, Tominaga T, Borlongan CV, Dezawa M. Transplantation of unique subpopulation of fibroblasts, Muse cells, ameliorates experimental stroke possibly via robust neuronal differentiation. Stem Cells. 2016; 34(1):160–173.
14. Uchida H, Niizuma K, Kushida Y, Wakao S, Tominaga T, Borlongan CV, Dezawa M. Human Muse cells reconstruct neuronal circuitry in subacute lacunar stroke model. Stroke. 2017;48(2):428–435.
15. Hosoyama K, Wakao S, Kushida Y, Ogura F, Maeda K, Adachi O, Kawamoto S, Dezawa M, Saiki Y. Intravenously injected human multilineage-differentiating stress-enduring cells selectively engraft into mouse aortic aneurysms and attenuate dilatation by differentiating into multiple cell types. J Thorac Cardiovasc Surg. 2018;155(6):2301–2313 e4.
16. Leng Z, Kethidi N, Chang AJ, Xu J, He X. Muse cells and neurorestoratology. J Neurorestoratol. 2019:in press.
17. Tsuchiyama K, Wakao S, Kuroda Y, Ogura F, Nojima M, Sawaya N, Yamasaki K, Aiba S, Dezawa M. Functional melanocytes are readily reprogrammable from multilineage-differentiating stress-enduring (Muse) cells, distinct stem cells in human fibroblasts. J Invest Dermatol. 2013;133(10): 2425–2435.
18. Yamasaki T, Wakao S, Kawaji H, Koizumi S, Sameshima T, Dezawa M, Namba H. Genetically engineered multilineage-differentiating stress-enduring cells as cellular vehicles against malignant gliomas. Mol Ther Oncolytics. 2017;6:45–56.
19. Yamada Y, Wakao S, Kushida Y, Minatoguchi S, Mikami A, Higashi K, Baba S, Shigemoto T, Kuroda Y, Kanamori H, Amin M, Kawasaki M, Nishigaki K, Taoka M, Isobe T, Muramatsu C, Dezawa M, Minatoguchi S. S1P-S1PR2 axis mediates homing of Muse cells into damaged heart for long-lasting tissue repair and functional recovery after acute myocardial infarction. Circ Res. 2018;122(8):1069–1083.
20. Wakao S, Akashi H, Kushida Y, Dezawa M. Muse cells, newly found non-tumorigenic pluripotent stem cells, reside in human mesenchymal tissues. Pathol Int. 2014;64(1):1–9.
21. Kuroda Y, Wakao S, Kitada M, Murakami T, Nojima M, Dezawa M. Isolation, culture and evaluation of multilineage-differentiating stress-enduring (Muse) cells. Nat Protoc. 2013; 8(7):1391–1415.
22. Uchida N, Kushida Y, Kitada M, Wakao S, Kumagai N, Kuroda Y, Kondo Y, Hirohara Y, Kure S, Chazenbalk G, Dezawa M. Beneficial effects of systemically administered human Muse cells in adriamycin nephropathy. J Am Soc Nephrol. 2017;28(10):2946–2960.
23. Abdelmawgoud H, Saleh A. Anti-inflammatory and antioxidant effects of mesenchymal and hematopoietic stem cells in a rheumatoid arthritis rat model. Adv Clin Exp Med. 2018; 27(7):873–880.
24. Alessio N, Squillaro T, Ozcan S, Di Bernardo G, Venditti M, Melone M, Peluso G, Galderisi U. Stress and stem cells: adult Muse cells tolerate extensive genotoxic stimuli better than mesenchymal stromal cells. Oncotarget. 2018;9(27): 19328–19341.
25. Araujo JAM, Hilscher MM, Marques-Coelho D, Golbert DCF, Cornelio DA, Batistuzzo de Medeiros SR, Leao RN, Costa MR. Direct reprogramming of adult human somatic stem cells into functional neurons using Sox2, Ascl1, and Neurog2. Front Cell Neurosci. 2018;12:155.
26. Balgi-Agarwal S, Winter C, Corral A, Mustafa SB, Hornsby P, Moreira A. Comparison of preterm and term Wharton's jelly-derived mesenchymal stem cell properties in different oxygen tensions. Cells Tissues Organs. 2018;205(3):137–150.
27. Barilani M, Banfi F, Sironi S, Ragni E, Guillaumin S, Polveraccio F, Rosso L, Moro M, Astori G, Pozzobon M, Lazzari L. Low-affinity nerve growth factor receptor (CD271) heterogeneous expression in adult and fetal mesenchymal stromal cells. Sci Rep. 2018;8(1):9321.
28. Durand-Herrera D, Campos F, Jaimes-Parra BD, Sanchez-Lopez JD, Fernandez-Valades R, Alaminos M, Campos A, Carriel V. Wharton's jelly-derived mesenchymal cells as a new source for the generation of microtissues for tissue engineering applications. Histochem Cell Biol. 2018;150(4):379–393.
29. Ebrahim N, Mostafa O, El Dosoky RE, Ahmed IA, Saad AS, Mostafa A, Sabry D, Ibrahim KA, Farid AS. Human mesenchymal stem cell-derived extracellular vesicles/estrogen combined therapy safely ameliorates experimentally induced intrauterine adhesions in a female rat model. Stem Cell Res Ther. 2018;9(1):175.
30. Ertl J, Pichlsberger M, Tuca AC, Wurzer P, Fuchs J, Geyer SH, Maurer-Gesek B, Weninger WJ, Pfeiffer D, Bubalo V, Parvizi D, Kamolz LP, Lang I. Comparative study of regenerative effects of mesenchymal stem cells derived from placental amnion, chorion and umbilical cord on dermal wounds. Placenta. 2018;65:37–46.
31. Liu H, Chen M, Liu L, Ren S, Cheng P, Zhang H. Induction of human adipose-derived mesenchymal stem cells into germ lineage using retinoic acid. Cell Reprogram. 2018;20(2): 127–134.

32. Nie W, Ma X, Yang C, Chen Z, Rong P, Wu M, Jiang J, Tan M, Yi S, Wang W. Human mesenchymal-stem-cells-derived exosomes are important in enhancing porcine islet resistance to hypoxia. Xenotransplantation. 2018: 25(5):e12405.
33. Wang YH, Yang ZQ, Zhu SF, Gao Y. Comparative study of methotrexate and human umbilical cord mesenchymal stem cell transplantation in the treatment of rheumatoid arthritis. J Biol Regul Homeost Agents. 2018;32(3):599–605.
34. Yamashita K, Inagaki E, Hatou S, Higa K, Ogawa A, Miyashita H, Tsubota K, Shimmura S. Corneal endothelial regeneration using mesenchymal stem cell derived from human umbilical cord. Stem Cells Dev. 2018;27(16):1097–1108.
35. Yang N, Ding Y, Zhang Y, Wang B, Zhao X, Cheng K, Huang Y, Taleb M, Zhao J, Dong WF, Zhang L, Nie G. Surface functionalization of polymeric nanoparticles with umbilical cord-derived mesenchymal stem cell membrane for tumor-targeted therapy. ACS Appl Mater Interfaces. 2018;10(27): 22963–22973.
36. Yu YB, Song Y, Chen Y, Zhang F, Qi FZ. Differentiation of umbilical cord mesenchymal stem cells into hepatocytes in comparison with bone marrow mesenchymal stem cells. Mol Med Rep. 2018;18(2):2009–2016.
37. Zhao D, Liu L, Chen Q, Wang F, Li Q, Zeng Q, Huang J, Luo M, Li W, Zheng Y, Liu T. Hypoxia with Wharton's jelly mesenchymal stem cell coculture maintains stemness of umbilical cord blood-derived CD34(+) cells. Stem Cell Res Ther. 2018;9(1):158.
38. Lim J, Razi ZR, Law J, Nawi AM, Idrus RB, Ng MH. MSCs can be differentially isolated from maternal, middle and fetal segments of the human umbilical cord. Cytotherapy. 2016; 18(12):1493–1502.
39. Amiri F, Halabian R, Salimian M, Shokrgozar MA, Soleimani M, Jahanian-Najafabadi A, Roudkenar MH. Induction of multipotency in umbilical cord-derived mesenchymal stem cells cultivated under suspension conditions. Cell Stress Chaperones. 2014;19(5):657–666.
40. An B, Na S, Lee S, Kim WJ, Yang SR, Woo HM, Kook S, Hong Y, Song H, Hong SH. Non-enzymatic isolation followed by supplementation of basic fibroblast growth factor improves proliferation, clonogenic capacity and SSEA-4 expression of perivascular cells from human umbilical cord. Cell Tissue Res. 2015;359(3):767–777.
41. Khatri M, Chattha KS. Replication of influenza A virus in swine umbilical cord epithelial stem-like cells. Virulence. 2015;6(1):40–49.
42. Trivanovic D, Jaukovic A, Popovic B, Krstic J, Mojsilovic S, Okic-Djordjevic I, Kukolj T, Obradovic H, Santibanez JF, Bugarski D. Mesenchymal stem cells of different origin: comparative evaluation of proliferative capacity, telomere length and pluripotency marker expression. Life Sci. 2015;141:61–73.
43. He H, Nagamura-Inoue T, Tsunoda H, Yuzawa M, Yamamoto Y, Yorozu P, Agata H, Tojo A. Stage-specific embryonic antigen 4 in Wharton's jelly-derived mesenchymal stem cells is not a marker for proliferation and multipotency. Tissue Eng Part A. 2014;20(7–8):1314–1324.
44. Kuroda Y, Dezawa M. Mesenchymal stem cells and their subpopulation, pluripotent muse cells, in basic research and regenerative medicine. Anat Rec (Hoboken). 2014;297(1):98–110.
45. Lee KS, Nah JJ, Lee BC, Lee HT, Lee HS, So BJ, Cha SH. Maintenance and characterization of multipotent mesenchymal stem cells isolated from canine umbilical cord matrix by collagenase digestion. Res Vet Sci. 2013;94(1):144–151.
46. Tunma S, Inthanon K, Chaiwong C, Pumchusak J, Wongkham W, Boonyawan D. Improving the attachment and proliferation of umbilical cord mesenchymal stem cells on modified polystyrene by nitrogen-containing plasma. Cytotechnology. 2013; 65(1):119–134.
47. Wakao S, Kuroda Y, Ogura F, Shigemoto T, Dezawa M. Regenerative effects of mesenchymal stem cells: contribution of muse cells, a novel pluripotent stem cell type that resides in mesenchymal cells. Cells. 2012;1(4):1045–1060.
48. Reza HM, Ng BY, Phan TT, Tan DT, Beuerman RW, Ang LP. Characterization of a novel umbilical cord lining cell with CD227 positivity and unique pattern of P63 expression and function. Stem Cell Rev. 2011;7(3):624–638.
49. Song H, Zhai X, Gao Z, Lu T, Tian Q, Li H, He X. Reliability and validity of a coda motion 3-D Analysis system for measuring cervical range of motion in healthy subjects. J Electromyogr Kines. 2018;38:56–66.
50. Dalamagkas K, Tsintou M, Seifalian A, Seifalian AM. Translational regenerative therapies for chronic spinal cord injury. Int J Mol Sci. 2018;19(6):E1776.
51. Kamalifar S, Azarpira N, Sadeghi L, Ghorbani-Dalini S, Nekoei SM, Aghdaie MH, Esfandiari E, Azarpira MR. ROCK Y-27632 inhibitor, ascorbic acid, and trehalose increase survival of human Wharton jelly mesenchymal stem cells after cryopreservation. Exp Clin Transplant. 2018.
52. Kim BE, Choi SW, Shin JH, Kim JJ, Kang I, Lee BC, Lee JY, Kook MG, Kang KS. Single-factor SOX2 mediates direct neural reprogramming of human mesenchymal stem cells via transfection of in vitro transcribed mRNA. Cell Transplant. 2018;27(7):1154–1167.
53. Wang S, Wang N, Cai Y, Wang H. Differentiation of human pluripotent stem cells into red blood cells. Sheng Wu Gong Cheng Xue Bao. 2018;34(6):983–992.
54. Suila H, Hirvonen T, Ritamo I, Natunen S, Tuimala J, Laitinen S, Anderson H, Nystedt J, Rabina J, Valmu L. Extracellular o-linked N-acetylglucosamine is enriched in stem cells derived from human umbilical cord blood. Biores Open Access. 2014; 3(2):39–44.
55. Feng YP, Sun TS, Chen L, Xie JX, Zhang ZC, Huang HY, He XJ, Chinese Assoc N, Chinese Branch Int Assoc N. Clinical therapeutic guideline for neurorestoration in spinal cord injury (Chinese version 2016). J Neurorestoratol. 2017;5:73–83.
56. Miltenyi S, Schmitz J. High gradient magnetic cell sorting. In: Radbruch A, ed. Flow Cytometry and Cell Sorting. Berlin, Heidelberg (Germany): Springer; 2000. p 218–247.
57. Richel DJ, Johnsen HE, Canon J, Guillaume T, Schaafsma MR, Schenkeveld C, Hansen SW, McNiece I, Gringeri AJ, Briddell R, Ewen C, Davies R, Freeman J, Miltenyi S, Symann M. Highly purified CD34+ cells isolated using magnetically

activated cell selection provide rapid engraftment following high-dose chemotherapy in breast cancer patients. Bone Marrow Transplant. 2000;25(3):243–249.
58. Kinoshita K, Kuno S, Ishimine H, Aoi N, Mineda K, Kato H, Doi K, Kanayama K, Feng J, Mashiko T, Kurisaki A, Yoshimura K. Therapeutic potential of adipose-derived SSEA-3-positive muse cells for treating diabetic skin ulcers. Stem Cells Transl Med. 2015;4(2):146–155.
59. Tian T, Zhang RZ, Yang YH, Liu Q, Li D, Pan XR. Muse cells derived from dermal tissues can differentiate into melanocytes. Cell Reprogram. 2017;19(2):116–122.
60. Gimeno ML, Fuertes F, Tabarrozzi AEB, Attorressi AI, Cucchiani R, Corrales L, Oliveira TC, Sogayar MC, Labriola L, Dewey RA, Perone J. Pluripotent nontumorigenic adipose tissue-derived Muse cells have immunomodulatory capacity mediated by transforming growth factor-beta 1. Stem Cells Transl Med. 2017;6(1):161–173.
61. Huang XP, Sun Z, Miyagi Y, Kinkaid HM, Zhang L, Weisel RD, Li RK. Differentiation of allogeneic mesenchymal stem cells induces immunogenicity and limits their long-term benefits for myocardial repair. Circulation. 2010;122(23): 2419–2429.
62. Alessio N, Ozcan S, Tatsumi K, Murat A, Peluso G, Dezawa M, Galderisi U. The secretome of Muse cells contains factors that may play a role in regulation of stemness, apoptosis and immunomodulation. Cell Cycle. 2017;16(1):33–44.
63. Amin M, Kushida Y, Wakao S, Kitada M, Tatsumi K, Dezawa M. Cardiotrophic growth factor-driven induction of human Muse cells into cardiomyocyte-like phenotype. Cell Transplant. 2018;27(2):285–298.
64. Hori E, Hayakawa Y, Hayashi T, Hori S, Okamoto S, Shibata T, Kubo M, Horie Y, Sasahara M, Kuroda S. Mobilization of pluripotent multilineage-differentiating stress-enduring cells in ischemic stroke. J Stroke Cerebrovasc. 2016;25(6):1473–1481.
65. Yamauchi T, Yamasaki K, Tsuchiyama K, Koike S, Aiba S. The potential of Muse cells for regenerative medicine of skin: procedures to reconstitute skin with muse cell-derived keratinocytes, fibroblasts, and melanocytes. J Invest Dermatol. 2017; 137(12):2639–2642.
66. Kurose R, Sawai T, Oishi K, Liu XZ, Sasaki A, Kurose A, Kumagai N, Fujishima Y, Ishibashi Y. Possibility of inhibiting arthritis and joint destruction by SSEA-3 positive cells derived from synovial tissue in rheumatoid arthritis. Regen Ther. 2017; 7:82–88.
67. Yabuki H, Wakao S, Kushida Y, Dezawa M, Okada Y. Human multilineage-differentiating stress-enduring cells exert pleiotropic effects to ameliorate acute lung ischemia-reperfusion injury in a rat model. Cell Transplant. 2018;27(6):979–993.